

AVALANCHES IN A NUMERICALLY SIMULATED SAND DUNE DYNAMICS

B. S. DAYA SAGAR,^{*,‡,§} M. B. R. MURTHY* and P. RADHAKRISHNAN†

**Faculty of Engineering and Technology (FET)*

†Faculty of Information Science and Technology (FIST)

Multimedia University, Melaka Campus

Jalan Ayer Keroh Lama, 75450, Melaka, Malaysia

‡bsdaya.sagar@mmu.edu.my

‡bsdsagar@hotmail.com

Received August 13, 2001

Accepted June 11, 2002

Abstract

Avalanches of various sizes occur due to instability during sand dune dynamics. A physically viable equation to model sand dune dynamics is a first order nonlinear difference equation. To visualize the size distribution of avalanches, sand dune dynamics has been numerically simulated by changing the strength of nonlinearity parameter (λ) that shows different impacts on dune dynamics. An equation to compute avalanche diameters, by considering the inter-slipface angles of a simulated sand dune under dynamics, is proposed. Using this equation, avalanche diameters have been computed from a dynamically changing simulated sand dune.

Keywords: Sand Dune; Fractal Dimension; Avalanche; Inter-Slipface Angle; Size Distribution.

1. INTRODUCTION

Windblown sand forms the dunes of various types. In a seminal work, Bagnold¹ discussed several aspects of dynamics of sand dunes. Since the introduction of the Bak-Tang-Wiesenfeld's concept of self-organized criticality (SOC),² a number of

automaton models have been developed to study avalanche dynamics.^{3–9} Lattice models of granular materials have previously been examined in many contexts; particularly in terms of self-organization and generalized in sandpiles.^{3–9} Coulomb noticed that a granular system with a slope of angle larger

[§]Corresponding author.

than an angle of repose would be unstable.¹⁰ A detailed scenario for the avalanches is discussed by deGennes.¹¹ Power law distribution of avalanche size-number has been studied by Herrmann¹² and Vandewalle.¹³ It is, however, interesting to model the distinct morphological dynamical behaviors of dunes. One of the equations that has the physical basis to model several possible morphological dynamical behaviors of dunes is the first order difference equation. Using this equation, numerical simulations have been carried out to understand the dune dynamical behaviors.¹⁴ This study¹⁴ has been further extended here to compute the number of avalanches of varied sizes by tuning the strength of nonlinearity parameter.

In what follows include the background and the associated information on the numerical simulation of morphological evolution of a sand dune, avalanches in this simulated sand dune, and a sample study by incorporating the numerically estimated avalanches and their statistics are given respectively in Secs. 2 to 4.

2. SIMULATION OF A SAND DUNE DYNAMICS

In case of continuous wind capable of transporting sand is available, the process of sand dune formation traverses several phase changes. The formation of a sand dune, of which the profile is like an ideal triangle, may be due to availability of convection and interferential types of wind capable of transporting sand to the supply area. In the present investigation, a profile of a sand dune with the following parameters has been considered.

2.1. Definition of Sand Dune Profile

The description of the morphology of a sand dune is concerned with its profile that is described as angular. The slipfaces of which are of equal lengths. A typical linear dune profile is shown in Fig. 1.

- Profile of dune should have a heap with two slipfaces of each length ($L_1 = L_2$). The profile is symmetric with respect to the origin at the center of the base of the dune.
- The width (d) of the base of the dune must be greater than the length of the slipface. This assumption is valid due to the fact that the length

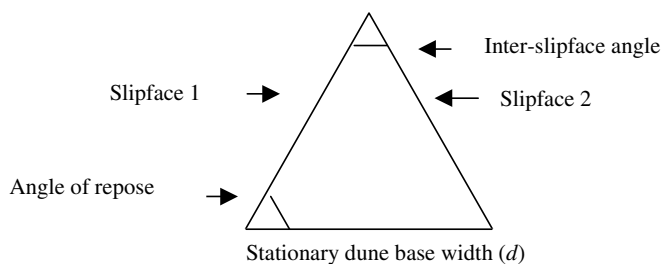


Fig. 1 Profile of a sand dune.

of the slipface is not greater than the width (d) in the case of real world dunes.

- Width of the dune is considered as rigid during the progressive dune evolution. However, the length of the slipface (L) varies with the continuous accretion of sand. Dune base length is stationary since the characteristic of supply area does not change. However, due to continuous sand supply, the slipface length tends to change, in turn the sand dune morphological dynamics. In other words, the slipface length is dynamic, whereas the base width is static. Inter-slipface angle is the diverging angle of a sand dune profile with two slipfaces. Characteristics of the simulated sand dune include that the profile of the dune has two slipfaces, hence an inter-slipface angle (θ), the base length (d), which is same for all the profiles of a dune under dynamics. The lesser the inter-slipface angle, the more is the height of the dune from the base and vice versa.

The degree of sand dune steepness can be quantified by fractal dimension.¹⁵ The shape of the generator¹⁵ incited us to use fractal dimension as a main parameter to simulate dune dynamics numerically, as the profile of which is compared with the generator morphologically. The fractal dimension is used as a main property of the sand dune undergoing dynamical changes. From the profile of a sand dune undergoing dynamics, the characteristics that substantiate the morphological constitution of sand dune at specific time interval include angle of repose, inter-slipface angle, dune height from the middle point of the sand dune base, and slipface lengths. The morphological dynamics of an ideal sand dune, of the type considered in the present study, can be modeled by considering any one (or) the combination of the characteristics. It is understood that by considering any two characteristics mentioned, one can derive the other characteristics. However, the fractal dimension of the profile of an

ideal sand dune is unified property from which one can define the other characteristics. For the profile of a sand dune, the normalized fractal dimension determines the steepness.

2.2. A Rule to Perform Numerical Simulation of Dune Morphological Dynamics by Incorporating Normalized Fractal Dimensions

If the slope of the dune is initially very small, only a few slides may occur, and so the dune will steepen. If the slope is very large, huge avalanches will sweep over the edges of the dunes and the slope will then become less steep. It is intuitively justifiable that the morphological changes in the sand dune is a nonlinear phenomenon, since the fractal dimensions of the successive profiles of a sand dune undergoing dynamics are not directly proportional to each other at successive time intervals. The intuitive argument may be endured by the fact that the sand dunes steepen and flatten over a time interval due to the distinct nature of sand dune structures. This argument may be supported by a postulate that the fractal dimension of successive profiles of a sand dune undergoing dynamics may be non-overlapping, and hence may be nonlinear. This phenomenon is due to the relatively divergent behavior of the sand that is accumulated, and also due to change in morphological constitution at discrete time intervals. It is intuitively apparent that the degree of unsteady state to fall over is more in the steep sand dune that possesses high fractal dimension. Hence, as the steepness of sand dune increases, the degree of fall over of sand becomes more when compared to the sand dune of lesser steepness. This phenomenon can be compared with *overcrowding* parameter in the context of population dynamics described in the logistic equations. This statement supports the argument that (α), the normalized fractal dimension tends to increase when it is small, and to decrease when it is large.

Several assumptions of the morphological dynamics seem to be cogent by the fact that the exo-dynamic processes, are always non-systematic that alter the morphological behavior of a sand dune. As the accretion process continues, several possible sand dune dynamical behaviors can be observed. To quantify these dynamical behaviors, of interest to certain geodynamicists, a first order nonlinear difference equation that has the physical viability

to simulate several dune dynamical behaviors has been adopted in earlier study.¹⁴ Certain equations, based on a first order nonlinear difference equation have been derived to estimate the attracting inter-slipface angles. The morphological dynamics of a sand dune profile, with two slipfaces and a fixed base length (d), has been modeled¹⁴ through bifurcation theory.¹⁶ The definition of a typical sand dune may be seen in the earlier works.^{14,17} To carry out computer (numerical) simulation to visualize distinct possible behaviors concerning a change in the strength of nonlinearity, a first order nonlinear difference Eq. (1), proposed elsewhere¹⁶ that has physical relevance in the simplest possible model to understand the formation, and several possible phase changes of a sand dune, undergoing dynamics, is considered as the basis.

$$\alpha_{t+1} = \lambda\alpha_t(1 - \alpha_t) \quad (1)$$

where α is the normalized fractal dimension of a sand dune profile, $0 \leq \alpha \leq 1$; and λ is the strength of regulatory parameter, $0 \leq \lambda \leq 4$.

The normalized fractal dimension α of the sand dune can be obtained by subtracting the topological dimension (D_T) from the fractal dimension as shown in Eq. (2).

$$\alpha = \left[\frac{\log(N)}{\log\left(\frac{d}{L}\right)} \right] - D_T \quad (2)$$

where

N = number of slipfaces (two for the present case);

d = width of the stationary base of the sand dune;

L = length of the slipface, $L \leq d$;

D_T = topological dimension;

α = normalized fractal dimension of a sand dune profile; and

$\alpha + D_T$ = fractal dimension (D)

A sand dune with a high degree of steepness will have a value of $\alpha = 1$, and with no steepness will have a value of $\alpha = 0$. Exo-dynamic processes will determine changes of a sand dune undergoing can be quantified by means of fractal dimension. Equation (1) has been studied extensively and is considered to be a simple model to explain the dynamics in one-dimensional maps, where increasing λ induces

period doubling bifurcation leading to chaos. This equation possesses one equilibrium point and the stability of the fixed point and the consequent dynamics exhibited by the systems are dependent on λ alone. To examine the long-term behavior of the sand dune morphology, or of fractal dimension of the dune profile, the Eq. (1), which has physical viability to understand the various phases is considered. In particular, we are interested in how this behavior depends upon the strength of nonlinearity parameter, λ . To keep the fractal dimensions of the profiles of a sand dune undergoing dynamics, and their corresponding inter-slipface angles between 180° and 90° , we limit our examination to values of λ between 0 and 4.

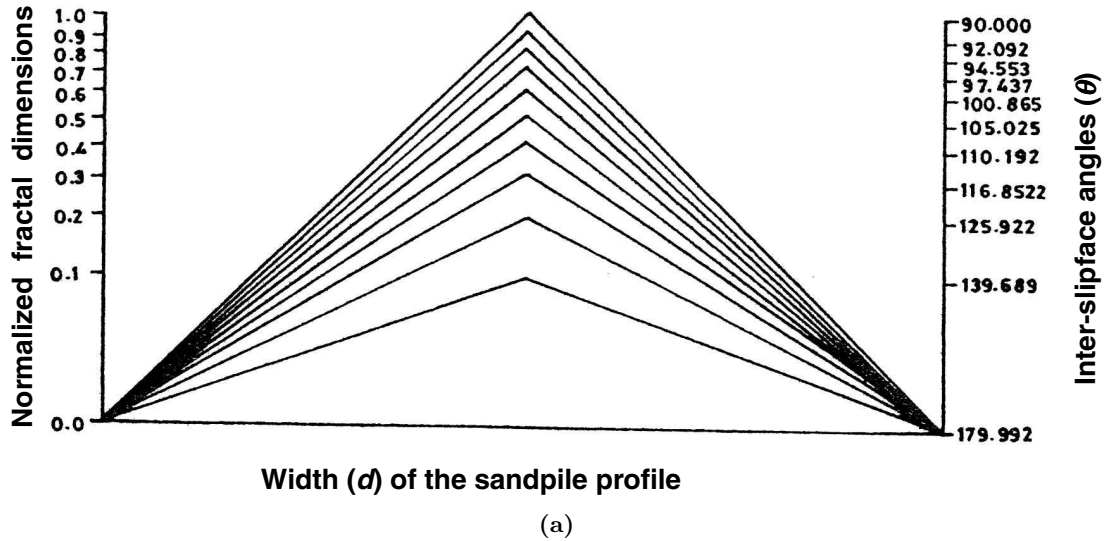
To study morphological dynamical behavior of a sand dune, it is necessary to know how much of the total morphological change is accommodated across time intervals. The rates of change in the fractal dimension of a dynamically changing sand dune at discrete time intervals depend upon the exo-dynamic processes. The collective impact of exo-dynamic processes (cause) which alter sand dune morphology can be defined as a strength of regulatory parameter by studying the (degree of deformation) effect due to the cause at discrete time intervals. As the fractal dimension enables the characteristic of the sand dune profile that is steepened as well as flattened, the parameter, λ can be defined as a numerical value. From the theoretical standpoint, the λ may be computed by considering the α_t and α_{t+1} to fit the curve $\lambda\alpha_t(1 - \alpha_t)$. This α gives the total description of the dynamics of sand dune. The impact of non-systematic exo-dynamic processes on a sand dune in terms of its dynamical behavior is investigated through the first order difference Eq. (1) of the form, $\alpha_{t+1} = f(\alpha_t)$; the normalized fractal dimension at $t + 1$, α_{t+1} is given as some function f of the α_t at time t . If this equation were linear (e.g. $f = \lambda\alpha$), α would just increase or decrease exponentially if $\lambda < 1$. Moreover, the fractal dimension tends to increase when at low α and to crash at high α value, corresponding to some nonlinear function with a hump of which the quadratic $f = \alpha_{t+1} = \lambda\alpha(1 - \alpha)$. It does mean, there is a tendency for the variable α to increase from time t to the next when it is small, and for it to decrease when it is large. This tendency is preserved due to the term $(1 - \alpha_t)$ in Eq. (1). In Eq. (1), to compute α_{t+1} , $\lambda\alpha_t(1 - \alpha_t)$ explains that the normalized status of sand dune dynamics in the case

of α starting at larger than 1, it immediately goes negative at one time step. If λ is less than 1, the sand dune is in a inhospitable environment that its fractal dimension diminishes at every discrete time interval. For values of λ below 1, the eventual fractal dimensions in normalized scale is zero of which the inter-slipface angle is zero (or it does not exist). Moreover, if $\lambda > 4$, the hump of the parabola exceeds 1, thus enabling the initial α value near 0.5 to exceed criticality in two time steps. Therefore, there is a need to restrict the analysis to values of λ between 1 and 4, and values of α between 0 and 1. In the qualitative understanding of dynamical behavior, value α_{t+1} is obtained from the previous value of α_t by multiplying it by $\lambda(1 - \alpha_t)$. It is clear that for $\lambda(1 - \alpha_t)$ to be greater than 1, the successive values, viz. α_{t+2} , α_{t+3} , α_{t+4} , \dots , α_{t+N} , will grow bigger, i.e. a change in α_t will get amplified. This is the sand dune steepness due to sand assemblage. If $\lambda(1 - \alpha_t)$ becomes smaller than 1, then subsequent values must diminish. This is sand dune flattening due to fall over of sand.

2.3. Relationship Between Normalized Fractal Dimension and Inter-Slipface Angle

As the sand dune crest reaches to critical inter-slipface angle, i.e. 90° (steepest of the sand dune) at which the normalized fractal dimension $\alpha = 1$, there is a tendency for α to decrease due to the fact that the unsteady state of sand to fall over is more in steeper sand dunes. On the contrary, when the sand dune profile possesses less fractal dimension, there may be a possibility for it to get steepened due to sand assemblage and due to more *sand holding* capacity in the supply area. When it possesses high fractal dimension, due to unsteady state to fall over is more and this may lead to a decline of the fractal dimension. However, it may also lead to oscillations, or even chaotic fluctuations depending on the nature of exo-dynamic processes, and the sand dune characteristics.

Equation (2), a part of which is due to Mandelbrot¹⁵ to compute fractal dimension of Koch generator that is similar to the sand dune profile, can be rewritten as Eq. (3). This equation computes the normalized fractal dimension of the sand dune profile by considering the inter-slipface angle. From the θ , the corresponding normalized fractal dimension can be calculated for the profile of a sand dune



Relation between normalized fractal dimension and inter-slipface angle

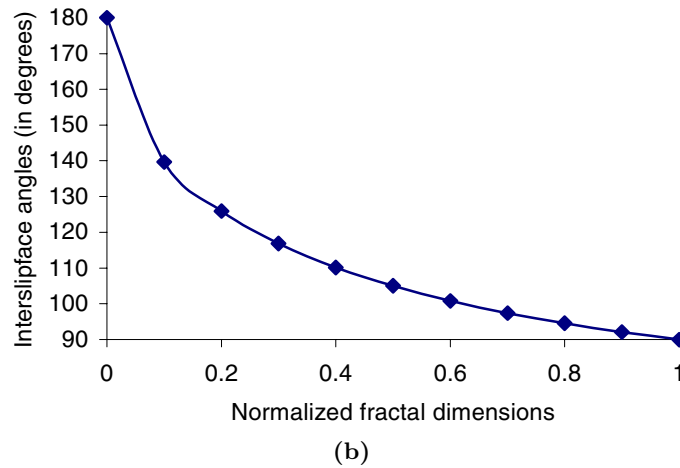


Fig. 2 (a) Sand dune profiles with different fractal dimensions and corresponding inter-slipface angles. (b) Graphical plot between the two parameters.

that has been considered by using Eq. (3).

$$\alpha = \left\{ \left[\frac{\log(N)}{\log \left[2 \sin \left(\frac{\theta}{2} \right) \right]} \right] - D_T \right\} \quad (3)$$

From Eq. (3), it can be understood that the profiles of the sand dunes with $\theta = 90^\circ$ (steepest) and $\theta = 180^\circ$ (zero-steepness) of inter-slipface angles possess normalized fractal dimensions 1 and 0, respectively. The simplest profile of a simple sand dune one could imagine is with two slipfaces ($N = 2$) making an angle θ that satisfies $90^\circ \leq \theta \leq 180^\circ$.

The limitcase $\theta = 180^\circ$ generates a dune at the initial state ($t = 0$); the case $\theta = 90^\circ$ generates a dune at the unstable state, the fractal dimension of which has been estimated as 1 (when $\theta = 180^\circ$) and 2 (when $\theta = 90^\circ$). For a better understanding, the profiles of a sand dune are illustrated with normalized fractal dimensions and their corresponding inter-slipface angles (Fig. 2).

Are there any sand dunes with repose angles of more than 45°?

Sand dunes may have the range of angles of repose from 10° to 45° depending upon the sand particle

properties such as shape, size and interlocking properties, which are subjected to change with exogenic nature of forces. This upper limit of the angle of repose, i.e. 45° incited us to consider the lower and upper limits of the normalized fractal dimensions and their corresponding inter-slipface angles within the range of $0 \leq \alpha \leq 1$ and $180^\circ \leq \theta \leq 90^\circ$, respectively. The upper limit of fractal dimension of the sand dune is 2, and the corresponding inter-slipface angle, and the angle of repose of which are, respectively, 90° and 45° . Since the upper limit of angle of repose is 45° , the validity of the range of fractal dimensions between $90^\circ \leq \theta \leq 180^\circ$ of sand dune with two slipfaces undergoing dynamics is reasonable and logical. In simple terms, if there exists a sand dune with angle of repose or inter-slipface angle, at any time as the sand dune undergoing dynamical changes, exceeds the limit of 45° (angle of repose) or 90° (inter-slipface angle), this simple model, where the normalized fractal dimension of

an ideal sand dune which has been considered as a unified quantity, fails.

2.4. Computation of Inter-Slipface Angle of a Sand Dune Under Dynamics

For the profile of a sand dune under dynamics with two slipfaces, the θ_{t+1} is a function of θ_t . Instead of α , one can consider θ values to carry out simulations for modeling. Equation (5) is proposed by considering Eqs. (1) and (3). In Eq. (5), the *ISFA* at time t is considered instead of the *NFD* to compute the *ISFAs* at time $t + 1, \dots, t + n$ of the sand dune undergoing dynamics according to first order difference equation as a dynamical rule. The *ISFAs* at time $t + 1$ can be computed by considering θ at time t as some function defined as follows

$$\theta_{t+1} = f(\theta_t). \quad (4)$$

The function is defined as

$$\theta_{t+1} = 2 \sin^{-1} \left\{ \frac{10^{\{\lambda \{\log N / [\log [2 \sin \theta_t / 2]] - D_T\} \frac{\log N}{\{1 - \{\log N / [\log [2 \sin \theta_t / 2]] - D_T\} + D_T\}}\}}}{2} \right\} \quad (5)$$

where θ_t and θ_{t+1} = inter – slipface angles at discrete times t and $t + 1$, respectively. The limits of various parameters are $0 < \alpha < 1$, $180^\circ > \theta > 90^\circ$, $1 < D < 2$.

Iterating Eq. (5) produces time series of inter-slipface angles (θ) of a simulated sand dune undergoing morphological changes dynamically. A one-dimensional map (Fig. 3) has been plotted by considering the time series of inter-slipface angles computed at $\lambda = 4$. This type of map enables the region of avalanche occurrence. This time series data can be used to compute the sizes of avalanches occurred. The inter-slipface angles computed by iterating the function, defined in Eq. (5), can be used to represent them in θ -space to visualize them in the form of a sand dune phase map.¹⁷

3. AVALANCHES IN A SIMULATED SAND DUNE

Up to some state of sand accretion process, no avalanches in the sand dune will occur. From the critical state, which can be determined by an angle of repose, the avalanches of several sizes will occur. As the steepness of sand dune increases, the possibility of avalanche occurrences will also increase. A

recipe to understand the sand dune dynamical behavior, while the sand supply is continuous, is that, a higher value for the normalized fractal dimension (α) of the sand dune profile at discrete time t than at time $t + 1$ is an indication of occurrence of an avalanche of a specific size. The avalanche size is computed as the distance between the two peaks, with a condition that the $\theta_{t+1} > \theta_t$, of successive profiles. This rolling starts from the state that the angle of repose of the dune reaches to critical state. The avalanche size is defined as the diameter of the out-scribed circle of the avalanche (Fig. 4). This schematic diagram shows the dune at two discrete time intervals with a possible avalanche. The avalanche size or diameter can be computed by the trajectory parts between the region of below the conditional bisectrix line and above the inverted parabola of the one-dimensional map shown in Fig. 3 indicate the occurrence of avalanches. The larger the length of the trajectory part in this region, the larger is the avalanche size.

$$\text{Avalanche size} = \frac{d}{2} \left\{ \left[\cot \left(\frac{\theta_t}{2} \right) \right] - \left[\cot \left(\frac{\theta_{t+1}}{2} \right) \right] \right\}. \quad (6)$$

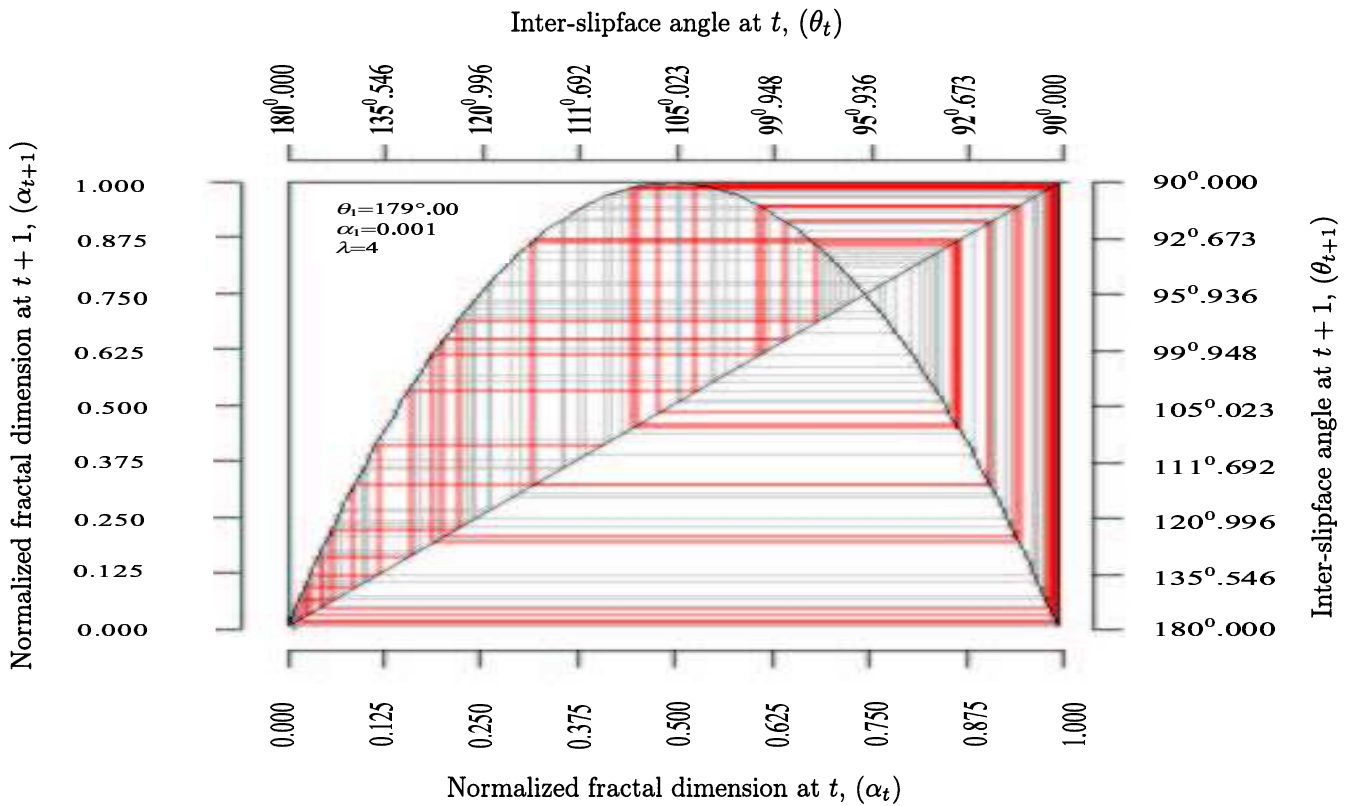


Fig. 3 A one-dimensional map plotted between θ_{t+1} vs. θ_t for sand dune case at $\lambda = 4$.

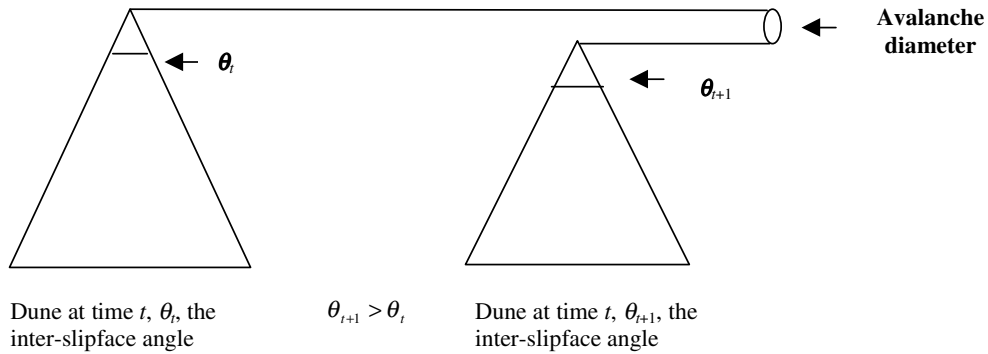


Fig. 4 Diameter of an avalanche. (The inter-slipface angles at discrete time intervals are shown with a possible avalanche since $\theta_{t+1} > \theta_t$.)

It will be considered that there is an avalanche of particular size only if $\theta_{t+1} > \theta_t$. The size of the avalanche depends on the difference between the θ values at successive discrete time intervals. In contrast, if the θ value is lesser than its preceding value in the time series data, then it will not be considered as an avalanche. However, it can be said that the sand dune steepens further.

4. SAMPLE STUDY AND RESULTS

The dune profiles and corresponding inter-slipface angles are generated in discrete time intervals. From these time series of inter-slipface angles, the distance between the two peaks of the successive dune profiles at discrete time intervals can be computed. From the simulated time series of embedded

θ values with a condition that $\theta_{t+1} > \theta_t$, the changing out-scribed diameter of an avalanche is computed by using Eq. (6). It is interesting to observe the number of avalanches of varied sizes by changing various parameters, in Eq. (5), such as λ , α and d . In Table 3, the size distribution of avalanches has been shown by changing d with $\lambda = 4$. These results are discussed.

4.1. Strength of Nonlinearity versus the Avalanche Size Distribution

It is worthwhile to study the relation between the strength of nonlinearity and the avalanche size distributions. To deal with this exercise, an unified diagram may be shown to understand the avalanche dynamics in this simulated sand dune dynamics. This simulated sand dune dynamics enables all possible behaviors of a sand dune that undergoes morphological changes with a given strength of nonlinearity. In the present model, the avalanches started observed at the angle of repose 37.4° . The sand dune under dynamics with a strength of nonlinearity 2.1 will attain critical state from which the avalanches are being observed, the angle of repose of such sand dune under dynamics is 37.4° .

- The avalanche count is found to increase and then decrease with an increase in strength of nonlinearity. As the strength of nonlinearity is increased, it is observed that the number of avalanche size categories has increased. It is also observed during the investigations that when the strength of nonlinearity is less than two, no avalanches were observed in this numerically simulated sand dune dynamics. Avalanche size distribution has been carried out by changing the λ and the results are given in Table 1.
- All slopes below some critical value seem to be stable. After some time, the shape does not change anymore and all additional grains just flow along the surface to the rim of the base where they fall off. While for spherical particles, it is reported that the angle of repose is typically 10° – 20° , dry sand exhibits $\sim 30^\circ$ – 40° and the humidity can make it rise much more. However, the computed angle of repose, from the model thus simulated, is 37.4° . This is in conformity with the specified range, i.e. 30° – 40° of angle of repose for the dry sand, proposed by Herrmann.⁷ From the study, it is inferred that the critical angle of repose is 37.4° .

This angle of repose will be attained when the strength of nonlinearity (λ) that has been used in the model is > 2 .

4.2. Classification of Dunes Based on Occurrence of Avalanches

Certain characteristics of the dune dynamics at threshold strength of nonlinearities have been given in Table 2.

- Stability of the sand dune is defined in terms of occurrence of avalanches. Continuous accretion of sand keeps the dune active. Such dunes are called *active dunes*. However, a dune is said to be *inactive*, if there are no avalanches after certain discrete time intervals. Due to absence of sand supply or winds capable of transporting sand, an *active dune* may turn into an *inactive dune*. In real case, such a phenomenon might arise after a long period. On the Mars, such *inactive dunes* that were once active can be seen. It is observed that for the strength of nonlinearity parameter $\lambda > 3$ dunes are active.
- From this numerically simulated sand dune dynamics, the dune dynamics are categorized, based on the avalanche occurrences with discrete time, as super-stable, semi-stable, and chaotically behaving dunes.
- Sand dunes behaviors can be visualized as phase changes. Conventionally, it has been defined that a sand dune will have one angle of repose. Once the dune reaches to this critical state, avalanches will be observed. However, it is also true that there may be numerous angles of repose in a sand dune undergoing dynamics. This can be schematically represented through a bifurcation diagram, i.e. we can argue this phenomenon of having different angles of repose in a sand dune undergoing dynamics as changing properties of sand. With changing sand properties, the interlocking parameters will be changed, hence the angle(s) of repose when the interlocking properties of sand particles (of a dune) change due to the reason that the sand characteristics are primarily subjected to exogenic nature of processes. In turn, the angle of repose is not just the one, there will be numerous angle(s) of repose as the sand dune undergoing dynamical changes. It is reported by several researchers that the angle of repose varies with the change in characteristics of sand particles, and also with the fluctuations in the

Table 1 Total avalanche count and avalanche distribution.

λ	Total Avalanche count	Distribution of avalanches according to diameters								
		<0.5 mts	0.5–1.0 mts	1.0–1.5 mts	1.5–2.0 mts	2.0–2.5 mts	2.5–3.0 mts	3.0–3.5 mts	3.5–4.0 mts	>4.0 mts
2.1	2	2	0	0	0	0	0	0	0	0
2.2	4	4	0	0	0	0	0	0	0	0
2.3	5	5	0	0	0	0	0	0	0	0
2.4	6	6	0	0	0	0	0	0	0	0
2.5	9	9	0	0	0	0	0	0	0	0
2.6	13	13	0	0	0	0	0	0	0	0
2.7	19	19	0	0	0	0	0	0	0	0
2.8	30	30	0	0	0	0	0	0	0	0
2.9	63	63	0	0	0	0	0	0	0	0
3.0	748	748	0	0	0	0	0	0	0	0
3.1	748	748	0	0	0	0	0	0	0	0
3.2	748	4	744	0	0	0	0	0	0	0
3.3	748	5	743	0	0	0	0	0	0	0
3.4	749	3	746	0	0	0	0	0	0	0
3.5	749	1	374	374	0	0	0	0	0	0
3.6	749	76	220	453	0	0	0	0	0	0
3.7	715	271	156	128	160	0	0	0	0	0
3.8	655	150	131	101	171	102	0	0	0	0
3.8	606	76	61	134	86	122	127	0	0	0
4.0	492	74	65	62	62	43	47	52	50	36

$\alpha = 0.1$; Dune base length = 9 mts; Number of iterations = 1500.

Table 2 Dune classification based on the occurrence of avalanches.

Threshold Strength of Nonlinearity (λ)	Occurrence of Avalanches during Active State of Dune	No. of Avalanches during Active State of Dune	Avalanche Diameter(s) in mts	Stability Type	Active/Inactive Over a Period of Time	No. of Angle(s) of Repose
2	No	0	0	Stable	In-active	Nil
3	Yes	748	0.027514	Initially period 2	In-active	One
3.46	Yes	749	1.086073 and 0.87355	Periodically changing	Active	Two
3.57	Yes	749	Many avalanches of various diameters ranging from 0.54 to 1.4	Chaotically changing	Hyper-active	Many

$\alpha = 0.1$; $d = 9$ mts; Iterations = 1500.

Table 3 Avalanche distribution.

Total Count	<0.5 mts	0.5–1.0 mts	1.0–1.5 mts	1.5–2.0 mts	2.0–2.5 mts	2.5–3.0 mts	3.0–3.5 mts	3.5–4.0 mts	>4.0 mts
<i>d</i> = 3 mts									
3905	1611	1154	1140	0	0	0	0	0	0
<i>d</i> = 6 mts									
3905	885	722	613	554	557	574	0	0	0
<i>d</i> = 9 mts									
3905	592	569	446	417	385	365	416	400	288

$\alpha = 0.1$; $\lambda = 4$; Iterations = 12,000.

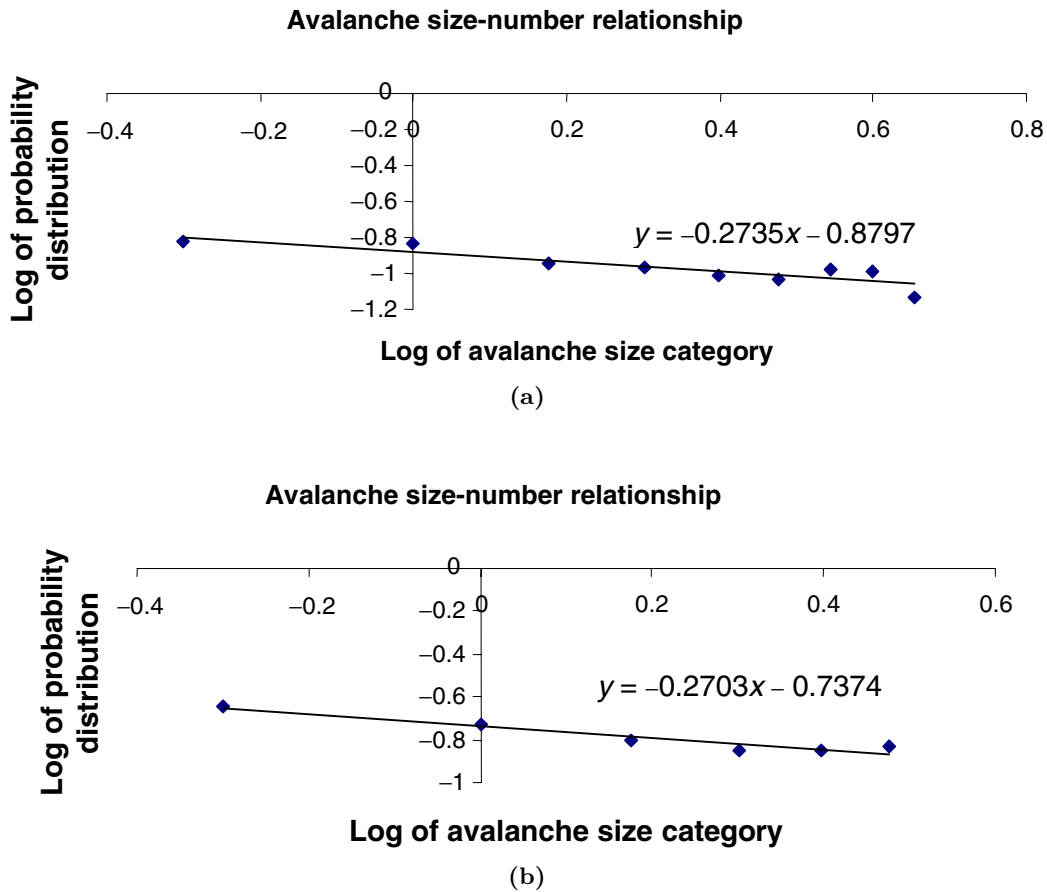


Fig. 5 Graphical plots between the logarithms of avalanche size and avalanche number for (a) dune width of 9 m and (b) dune width of 6 m.

wind strength. It can be said that these characteristic changes may be due to exogenic nature of processes in general. There will be an angle of repose variation during the process of sand dune dynamics. Dune changes its phases with dynamically varying sand particle interlocking proper-

ties, strength of wind, etc. While traversing several phase changes, a dynamically changing dune possesses one or more angles of repose. It is observed that the avalanche diameter gets reduced with discrete time for the strength of nonlinearity $2 < \lambda \leq 3$. As the iterative process is progressing,

the dune becomes stable for the strength of nonlinearity between 2.1 and 3. Avalanches of fixed sizes are observed with a periodic interval for the strength of nonlinearity $3 < \lambda \leq 3.46$. It is interesting to note that the avalanches of two different diameters are observed periodically when the strength of nonlinearity is $3.46 \leq \lambda < 3.57$. Such a case can be visualized when the strength of nonlinearity is in the range $3.46 \leq \lambda < 3.57$. For the strength of nonlinearity > 3.57 , the avalanche diameter and number distributary pattern is chaotic. The number of angle(s) of repose vary with the strength of nonlinearity, of a dynamically changing simulated sand dune and has (have) been given in Table 2.

4.3. Avalanche Distribution in Different Sizes of Dunes

Results with stationary base lengths of 3, 6 and 9 mts with initial normalized fractal dimension of 0.1, and number of iterations of 12,000 have been given in Table 3 to understand the distributary pattern of avalanche diameter number of a chaotically behaving sand dune.

- It is observed that the total avalanche count remains the same in spite of a change in the base length. Graphs have been plotted between the avalanche size versus number for the sand dunes with base width of 9 m and 6 m [Figs. 5(a) and (b)]. No significant variation has been found in these graphs. However, the distributed avalanche count varies.
- For 3 m base length avalanches up to 1.5 m, while for 6 m base length, the avalanche size up to 3 m, and it is more than 4 m for 9 m base length were observed.
- The number of avalanches of a specific size reduces as the base length is increased.
- With base lengths 6 m and 9 m, it is observed that the number of avalanches of different diameters initially reduces, reaches a minimum, and then increases again before the process extincts.

5. CONCLUSION

This study of theoretical interest can be considered to validate by incorporating the inter-slipface angles, of corresponding profiles of a real world

sand dune undergoing dynamics, the retrieval of which is possible with the advent of the availability of multi-temporal, high resolution interferometrically generated digital elevation models (DEMs) at different time-scales. Certain geodynamic problems such as the morphological evolutionary behavior of a sand dune can be better modeled by using the multi-date DEMs, derived from high resolution remotely sensed data. From such a study, one can understand the distribution of avalanches of real world sand dunes of various sizes undergoing dynamics.

ACKNOWLEDGMENTS

The authors are grateful to the two anonymous reviewers for providing their valuable comments and suggestions which help further improve the manuscript.

REFERENCES

1. R. A. Bagnold, *Physics of Wind Blown Sand and Sand Dunes* (Methuen, 1941).
2. P. Bak, C. Tang and K. Wiesenfeld, *Phys. Rev. Lett.* **59**, 381 (1987).
3. N. Vandewalle and M. Ausloos, *Comp. Graph.* **20**, 921 (1996).
4. Y. C. Zhang, *Phys. Rev. Lett.* **63**, 470 (1989).
5. H. Takayasu, *Phys. Rev. Lett.* **63**, 2563 (1989).
6. D. Dhar, *Phys. Rev. Lett.* **64**, 1613 (1990).
7. V. B. Priezhennev, A. Dhar, S. Krishnamurthy and D. Dhar, *Phys. Rev. Lett.* **77**, 5079 (1996).
8. D. Dhar, *Physica* **A263**, 4 (1999).
9. L. P. Kadanoff, S. R. Nagel, L. Wu and S.-M. Zhou, *Phys. Rev.* **A39**, 6254 (1989).
10. R. Nedermann, *Statics and Kinematics of Granular Materials* (Cambridge University Press, London, 1992).
11. P. G. deGennes, *Physica* **A261**, 267 (1998).
12. H. J. Herrmann, *Physica* **A270**, 82 (1999).
13. N. Vandewalle, *Physica* **A272**, 4508 (1999).
14. B. S. D. Sagar, *Chaos, Solitons & Fractals* **10**(9), 1559 (1999).
15. B. B. Mandelbrot, *Fractal Geometry of Nature* (Freeman, New York, 1982).
16. R. M. May, *Nature* **261**, 459 (1976).
17. B. S. D. Sagar and M. Venu, *Discrete Dynamics in Nature and Society* **6**(1), 64 (2001).